Preparation, Structure, and Amphoteric Redox Properties of *p*-Phenylenediamine-Type Dyes Fused with a Chalcogenadiazole Unit

Takanori Suzuki* and Takashi Tsuji

Division of Chemistry, Graduate School of Science, Hokkaido University, Sapporo 060-0810, Japan

Tsuneyuki Okubo, Akihisa Okada, Yoshiaki Obana, Takanori Fukushima, and Tsutomu Miyashi

Department of Chemistry, Graduate School of Science, Tohoku University, Aoba-ku, Aramaki, Sendai 980-8578, Japan

Yoshiro Yamashita

Department of Electronic Chemistry, Interdisciplinary Graduate School of Science and Engineering, Tokyo Institute of Technology, Yokohama 226-8502, Japan

tak@sci.hokudai.ac.jp

Received August 9, 2001

4,7-Bis(dialkylamino)benzo[*c*][1,2,5]chalcogenadiazoles are a novel class of organic dyes that undergo reversible two-stage one-electron oxidation as well as one-electron reduction. They exhibit absorption maxima in the long-wavelength region, which are assigned as intramolecular charge transfer bands from the phenylenediamine moiety to the electron-accepting heterocycle. Their redox properties as well as molecular and crystal structures are affected by the alkyl substituents on the amino nitrogen and/or by the chalcogen atom (O, S, Se) in the heterocycle.

Recently, much attention has been focused on organic redox systems due to their special properties such as their conducting behavior and ferromagnetism.[1] We designed the title molecules, 4,7-bis(dialkylamino)benzo[*c*][1,2,5]-chalcogenadiazoles (**1**−**3**(**a**,**b**)), as novel Wurster-type electron donors,[2] which show several interesting features by annelation of an electron-withdrawing chalcogenadiazole ring:[3] (1) in addition to their strong donating properties inherent to the tetramethyl-*p*-phenylenediamine (TMPD)[4a] or 1,4-bis(1-pyrrolidinyl)benzene (BPB)[4b] skeleton, they also undergo one-electron reduction within an easily accessible potential window; (2) they exhibit strong absorptions in the visible region by intramolecular charge transfer (CT) from the phenylenediamine moiety to the heterocycle; and (3) their packing arrangement in crystal form may be affected by electrostatic interaction through short contacts between heteroatoms, which has been shown to be favorable for giving conducting organic solids.[5]

We report here the preparation and properties of **1**−**3**(**a**,**b**), along with the effects of the chalcogen atom (X = O, S, Se) on their amphoteric redox properties and crystal structures. The effects of alkyl substituents on amino nitrogens (N_{amino}) are also discussed by comparing two series of compounds with dimethylamino (**a**) and pyrrolidinyl groups (**b**).

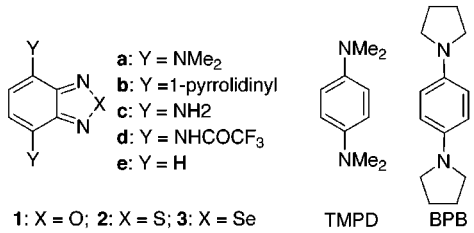

Results and Discussion

Preparation. 4,7-Bis(dimethylamino)benzo[*c*][1,2,5]-oxadiazole (**1a**) was prepared in 67% yield by *N*-methylation[6] of the corresponding free diamine **1c** with HCHO−$NaBH_4$. 4,7-Bis(1-pyrrolidinyl) derivative **1b** was also obtained from **1c** in 19% yield by treating the trifluoroacetylated compound **1d** with 1,4-dibromobutane/KOH[7] (Scheme 1). Similarly, the thiadiazole derivatives **2a** and **2b** were prepared from **2c** in respective yields of 94 and 59%. The diamine **2c** is also a new compound and was obtained in 65% yield by reacting 4-aminobenzothiadiazole (**4c**) with *p*-N_2^+-C_6H_4-SO_3^- followed by reduction of the azo dye with $Na_2S_2O_4$ (Scheme 2).

* Corresponding author. Fax: +81-11-706-4924.

(1) Bryce, M. R. *Adv. Mater.* **1999**, *11*, 11.
(2) Deuchert, K.; Hünig, S. *Angew. Chem., Int. Ed Engl.* **1978**, *17*, 875.
(3) Sherman, E. O.; Lambert, S. M.; Pilgram, K. *J. Heterocycl. Chem.* **1977**, *11*, 763.
(4) (a) Nelsen, S. F.; Tran, H. Q.; Nagy, M. A. *J. Am. Chem. Soc.* **1998**, *120*, 298. Roth, H. D. *Tetrahedron* **1986**, *42*, 6097. (b) Leonard, N. J.; Sauers, R. R. *J. Org. Chem.* **1956**, *21*, 1187.
(5) Suzuki, T.; Kabuto, C.; Yamashita, Y.; Mukai, T.; Miyashi, T.; Saito, G. *Bull. Chem. Soc. Jpn.* **1988**, *61*, 483. Iwasaki, K.; Ugawa, A.; Kawamoto, A.; Yamashita, Y.; Yakushi, K.; Suzuki, T.; Miyashi, T. *Bull. Chem. Soc. Jpn.* **1992**, *65*, 3350. Yamashita, Y.; Tanaka, S.; Imaeda, K.; Inokuchi, H.; Sano, M. *J. Org. Chem.* **1992**, *57*, 5517. Ono, K.; Tanaka, S.; Imaeda, K.; Yamashita, Y. *Chem. Commun.* **1994**, 899.
(6) Giumanini, A. G.; Chiaveri, G.; Musiani, M. M.; Rossi, P. *Synthesis* **1980**, 743.
(7) Johnstone, R. A. W.; Payling, D. W.; Thomas, C. *J. Chem. Soc. C* **1969**, 2223.

10.1021/jo010808h CCC: $20.00
Published on Web 11/30/2001

Scheme 1

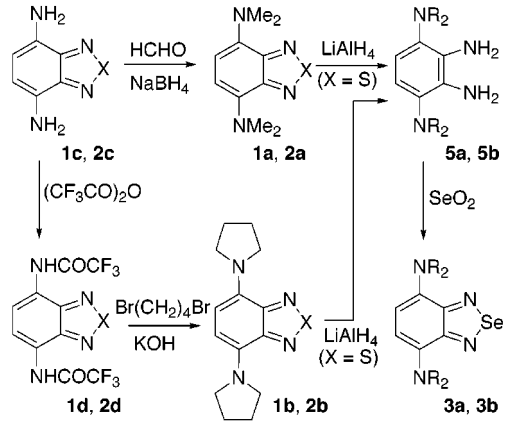

[**1**: X = O; **2**: X = S; **3**: X = Se; **a**: R = Me; **b**: R,R = -$(CH_2)_4$-]

Scheme 2

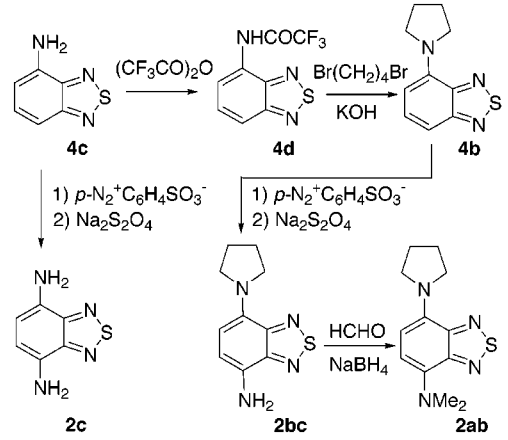

Reductive ring opening[8] of the thiadiazole ring in **2a** and **2b** by $LiAlH_4$ gave air-sensitive tetramines **5a** and **5b**, respectively, from which the selenadiazole derivatives **3a** and **3b** were prepared by treatment with SeO_2 in yields of 45 and 34% in two steps (Scheme 1). Unsymmetrically alkylated diamine **2ab** which has both dimethylamino and pyrrolidinyl groups was also prepared in a stepwise manner as shown in Scheme 2. All of the bis(dialkylamino)benzochalcogenadiazoles (**1**−**3**(**a**,**b**)) could be isolated as light- and air-stable crystalline materials with a deep red to violet color.

Molecular Structures. To determine the precise geometries of the newly prepared electron donors, single-crystal X-ray structural analyses were carried out at −150 °C for the thiadiazole derivatives **2a** and **2b**. The crystallographic study was also conducted on **2e**,[9] which does not have any amino groups. Inspection of the bond distances in **2e** shows that the benzothiadiazole skeleton exhibits pronounced bond alternation (Figure 1) as previously suggested by NMR spectroscopy.[12] Comparisons of π-bond orders[13] with dimethylamino derivative **2a** clearly show that the degree of bond alternation in the six-membered ring is larger in **2a** than in the parent

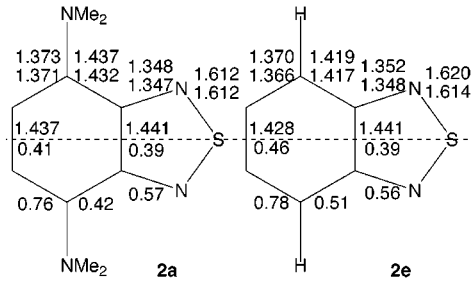

Figure 1. Bond lengths (R) of **2a** and **2e** determined by X-ray analyses at −150 °C (upper) and π-bond orders (p) (lower) calculated using the following equations: R/Å = 1.514 − 0.188p for C−C; R/Å = 1.443 − 0.167p for C−N.[11] Estimated standard deviations for bond lengths are 0.003−0.005 Å for **2a** and 0.002−0.004 Å for **2e**.

Scheme 3

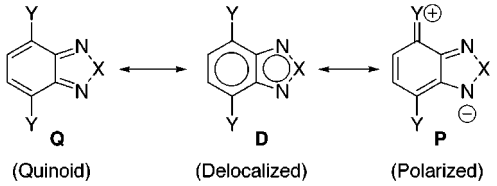

heterocycle **2e**. This result may be accounted for by the reduced contribution of the delocalized form (**D** in Scheme 3) due to the introduction of strong electron-donating groups[15] and may indicate an only small contribution of the polarized structure (**P**) in the ground state of **2a**. This seems to also be true for pyrrolidinyl derivative **2b**, although detailed comparisons are inappropriate due to the relatively large errors (0.01 Å) for the bond distances in **2b**.

A marked difference between **2a** and **2b** is found in the geometry around N_{amino}. In both cases, one of the two alkyl carbons on N_{amino} is located nearly in the same plane as benzothiadiazole. However, the other alkyl carbon close to the inimo nitrogen deviates from this plane; the deviation is much greater in dimethylamino derivative **2a** (1.25 and 1.29 Å) than in pyrrolidinyl derivative **2b** (0.80 and 0.91 Å). Such differences may be due to the greater steric requirements of the methyl compared to the methylene in the pyrrolidinyl group. On the other

(8) Mataka, S.; Takahashi, K.; Imura, T.; Tashiro, M. *J. Heterocycl. Chem.* **1982**, *19*, 1481.

(9) While X-ray structure of **2e** has been reported previously,[10] it was reanalyzed here to obtain precise bond distances with a sufficient accuracy (esd < 0.004 Å).

(10) Luzzati, V. *Acta Crystallogr.* **1951**, *4*, 193.

(11) Häfelinger, G. *Chem. Ber.* **1970**, *103*, 2902.

(12) Brown, N. M.; Bladon, P. *Spectrochim. Acta* **1968**, *24A*, 1869.

(13) π-Bond orders were calculated by using the established relationship, where the parameters were defined to fit hetero-π-systems containing carbon−nitrogen bonds.[11] The equations shown in the caption of Figure 1 were successfully used to analyze the geometrical features of thiadiazine and selenadiazine derivatives.[14]

(14) Gieren, A.; Lamm, V.; Haddon, R. C.; Kaplan, M. L. *J. Am. Chem. Soc.* **1979**, *101*, 7277; *J. Am. Chem. Soc.* **1980**, *102*, 5070.

(15) In the X-ray analyses on *p*-phenylenediamines, the C^1—C^2 bond (d_{12}) and its equivalents were longer than the standard of C^{Ar}—C^{Ar}, whereas the C^2—C^3 bond and its equivalents (d_{23}) tended to be shortened. For example, d_1 in tetrakis(2-pyridylmethyl)-*p*-phenylenediamine are 1.403(2) and 1.402(2) Å, and much longer than d_2 [1.380(2) Å].[16] In the case of tetraisopropyl-*p*-phenylenediamine, crystallographic studies were conducted at 150 K on the two rotational isomers around the N_{amino}—C^{Ar} bond; the dihedral angle between the N_{amino} lone pair and the benzene π system is 28 and 74° in monoclinic and triclinic modifications, respectively. The larger interaction between the N_{amino} lone pair and the π-system in the former induces a significant difference between d_{12} and d_{23} (d_{12}, 1.400, 1.402, 1.403, 1.404 Å; d_{23}, 1.387, 1.388 Å), whereas d_{12} and d_{23} are nearly equal in the latter modification (d_{12}, 1.398, 1.395 Å; d_{23}, 1.392 Å)[17] (esd of bond length 0.001−0.005 Å).

(16) Buchen, T.; Hazell, A.; Jessen, L.; McKenzie, C. J.; Nielsen, L. P.; Pederson, J. Z.; Schollmeyer, D. *J. Chem. Soc., Dalton Trans.* **1997**, 2697.

(17) Bock, H.; Göbel, I.; Näther, C.; Havlas, Z.; Gavezzotti, A.; Filippini, G. *Angew. Chem., Int. Ed. Engl.* **1993**, *32*, 1755.

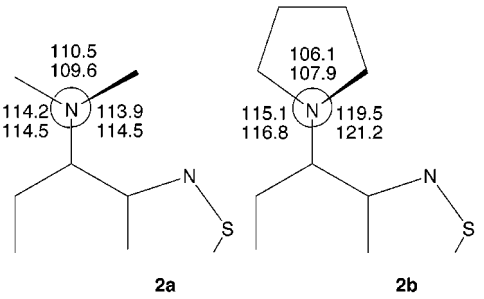

Figure 2. Angular geometry around amino nitrogens of **2a** (a) and **2b** (b). Estimated standard deviations for bond angles are 0.1−0.3° for **2a** and 0.4−0.7° for **2b**.

Table 1. Oxidation (E^{ox}) and Reduction Potentials ($E^{red.}$)[a] and the Lowest-Energy Absorption Maxima (λ_{max}) for 1−3 and Related Compounds in MeCN

compd	E_1^{ox}/V	E_2^{ox}/V	$E_1^{red.}$/V	E_{sum}/V[b]	λ_{max}/nm
Y = NM_2					
1a (X = O)	+0.24	+0.68	−1.73[c]	1.97	476
2a (X = S)	+0.19	+0.58	−1.72[c]	1.91	478
3a (X = Se)	+0.15	+0.47	−1.57[c]	1.72	512
TMPD	+0.10	+0.67	<−2.0		331
Y = 1-pyrrolidinyl					
1b (X = O)	+0.09	+0.62	−1.79	1.88	522
2b (X = S)	−0.02	+0.50	−1.82	1.80	532
3b (X = Se)	−0.05	+0.42	−1.62	1.57	580
BPB	−0.02	+0.61	<−2.0		346
Y = H					
1e (X = O)	>+2.3		−1.48		301
2e (X = S)	>+2.3		−1.53		310
3e (X = Se)	+2.15[d]		−1.30	3.45	330

[a] *E*/V vs SCE, 0.1 mol dm^{-3} Et_4NClO_4 in MeCN, Pt electrode, scan rate 100 mV s^{-1}. [b] E_{sum} is defined as $E_1^{ox} - E_1^{red.}$. [c] Quasi-reversible waves. [d] Irreversible wave.

hand, the sums of the bond angles around N_{amino} are 338.6 and 338.6° in **2a**, whereas those in **2b** are much larger (345.9 and 340.6°) (Figure 2). By considering the ideal values of 328.4 and 360.0° for pure sp^3 and sp^2 nitrogens, respectively, the observed angles suggest that the N_{amino} lone pair has 18% s-character in **2a**, whereas that in **2b** is 15%. Such geometric and hybridization differences for N_{amino} may be responsible for the generally greater electron-donating properties of pyrrolidinyl derivatives (**b**) than dimethylamino derivatives (**a**) (vide infra).

Redox Properties. Redox potentials of **1**−**3**(**a**,**b**) measured by cyclic voltammetry in MeCN are shown in Table 1. All of them undergo reversible two-stage one-electron oxidation. They are strong electron donors such as TMPD and BPB, and their first oxidation potentials (E_1^{ox}) are even lower than that of the well-known donor tetrathiafulvalene (+0.36 V) measured under the same conditions. In both the dimethylamino series (**a**) and pyrrolidinyl series (**b**) of compounds, oxadiazole derivatives **1a** and **1b** are the weakest donors due to the strong electron-withdrawing nature of the C=N−O unit.[18a]

Consistent with the lower s-character of the N_{amino} lone pair in the pyrrolidinyl group than in the dimethylamino group, E_1^{ox} of **1**−**3**(**b**) are considerably lower than those of **1**−**3**(**a**) with the same chalcogen atom. The difference (0.15−0.21 V) is larger than expected based on a comparison of TMPD and BPB (0.12 V). This result can be accounted for by assuming a less coplanar arrangement of the dimethylamino lone pair with the π-system for steric reasons. The oxidation potentials of hybrid compound **2ab** (E_1^{ox} = +0.09 V, E_2^{ox} = +0.54 V) are intermediate between those of **2a** and **2b**, indicating that the donating effects of N_{amino} are additive in these compounds.

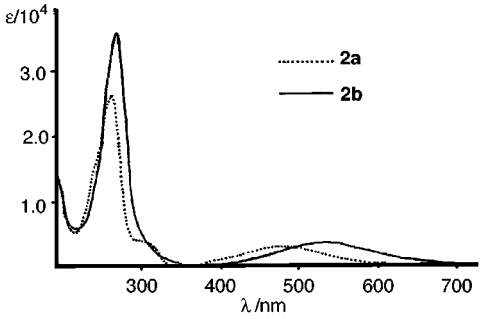

Figure 3. UV−vis spectra of **2a** and **2b** measured in MeCN.

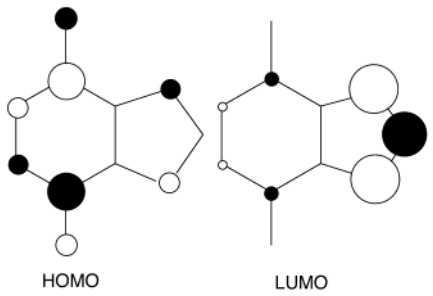

Figure 4. HOMO and LUMO of **2c** calculated by the HMO method. The areas of circles are proportional to the squares of LCAO coefficients.

Another interesting feature is the reversible one-electron reduction of **1**−**3**(**a**,**b**) within an easily accessible potential window, which reflects their electrochemical amphotericity. Selenadiazole derivatives **3a** and **3b** show the highest first reduction potential ($E_1^{red.}$) among each series of compounds, so that their amphotericities are also highest, as shown by the smallest E_{sum} values ($E_{sum} \equiv E_1^{ox} - E_1^{red.}$). This result is consistent with the finding that **3e** has the strongest electron-accepting ability among the parent heterocycles **1**−**3**(**e**) (Table 1), and **3e** itself shows electrochemical amphotericity due to the large polarizability of the selenium atom.

Intra- and Intermolecular Charge Transfer (CT). While TMPD, BPB, and unsubstituted benzochalcogenadiazoles **1**−**3**(**e**) show absorption only in the UV region (Table 1), all of the bis(dialkylamino)benzochalcogenadiazoles **1**−**3**(**a**,**b**) exhibit strong absorption (log ϵ, ca. 3.5) in the visible region, which reaches up to 600−700 nm (Figure 3). These broad absorption bands were assigned to a HOMO−LUMO transition, since the positions of absorption maxima correlate with E_{sum} values. Thus, λ_{max} of selenadiazole derivatives **3a** and **3b**, which have the highest amphotericity, are the longest in the dimethylamino (**a**) and pyrrolidinyl (**b**) series, respectively.

According to the HMO calculation for **2c**, the MO coefficients are large at the diaminodiene moiety in its HOMO, whereas the coefficients are nearly localized on the heterocycle in its LUMO (Figure 4). Thus, the lowest-energy bands in **1**−**3**(**a**,**b**) are characterized as intramolecular CT absorptions from the strongly donating amino

(18) (a) Suzuki, T.; Yamashita, Y.; Fukushima, T.; Miyashi, T. *Mol. Cryst. Liq. Cryst.* **1997**, *296*, 165. (b) Suzuki, T.; Fujii, H.; Yamashita, Y.; Kabuto, C.; Tanaka, S.; Harasawa, M.; Mukai. T.; Miyashi, T. *J. Am. Chem. Soc.* **1992**, *114*, 3034.

groups to the electron-deficient heterocycle. The lack of dependence of the molar absorption coefficient on the concentration also supports the intramolecular nature of this band [ϵ of **3a** at 512 nm: 2417 (3.01×10^{-4} mol dm^{-3}), 2401 (1.51×10^{-4} mol dm^{-3}), and 2458 (7.53×10^{-5} mol dm^{-3})].

When a solution of these diamines was combined with a strong electron acceptor, intermolecular CT was induced to give crystalline CT complexes. Although **2a** did not form any solid-state complex with tetracyanoquinodimethane (TCNQ; E_1^{red}, +0.18 V), admixing with the heterocyclic acceptors, 1,2,5-thiadiazolo-TCNQ (MTDA)[18a] and bis[1,2,5]thiadiazolo-TCNQ (BTDA),[18b] gave a green-black powder of complexes with a donor-to-acceptor molar ratio of 1:1. They exhibit electrical conductivities (σ) of 5.8×10^{-6} and 1.3×10^{-2} S cm^{-1}, respectively. Higher conductivity in the latter may be accounted for by the partial CT state[19] in **2a**-BTDA, whereas **2a**-MTDA would exhibit complete CT due to the stronger electron affinity of MTDA ($E_1^{red.}$, +0.12 V) than of BTDA (−0.02 V). Other complexes [**1a**-MTDA (molar ratio, 1:2; $\sigma = 4.5 \times 10^{-3}$ S cm^{-1}); **1a**-BTDA (2:3; 1.2×10^{-3}); **3a**-BTDA (1:1; 6.7×10^{-3})] were obtained by the similar direct combination of the diamine and the acceptor. Their conductivities are not spectacular but comparable to those reported for CT complexes of aromatic diamines.[20]

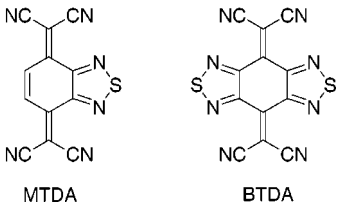

Crystal Structures. To obtain information on the factors that affect the molecular packing of diaminobenzochalcogenadiazoles, characteristic features of the crystal structures of **2a** and **2b** were investigated. In contrast to other redox systems containing a thiadiazole unit,[5] there are no short interheteroatom contacts such as S···N in either **2a** or **2b**. Since S···N contacts are present even in the parent heterocycle **2e**,[10] the introduction of an amino group at the 4,7-positions must suppress such interaction. Instead, one-dimensional columnar stacks are found in both **2a** and **2b** (Figure 5), in which the molecules are arranged in parallel with a slipped face-to-face overlap. Thus, the $\pi-\pi$ interaction seems the governing factor in determining the crystal structures of **2a** and **2b**. By considering the MO coefficients (Figure 4 for **2c**), these overlaps are not suitable for HOMO−LUMO interaction, indicating that the $\pi-\pi$ interaction observed here is mainly electrostatic in nature.[21]

Interheteroatom interaction through Se···N contacts has been shown to be much stronger than that through S···N.[14,18] X-ray analysis was also carried out on the selenadiazole derivative **3a**.[22] While **3a** has the same molecular framework to **2a**, there is no face-to-face π-stacking in **3a**. However, two kinds of very short Se···N_{amino} contacts are observed (3.26 and 2.98 Å; sum

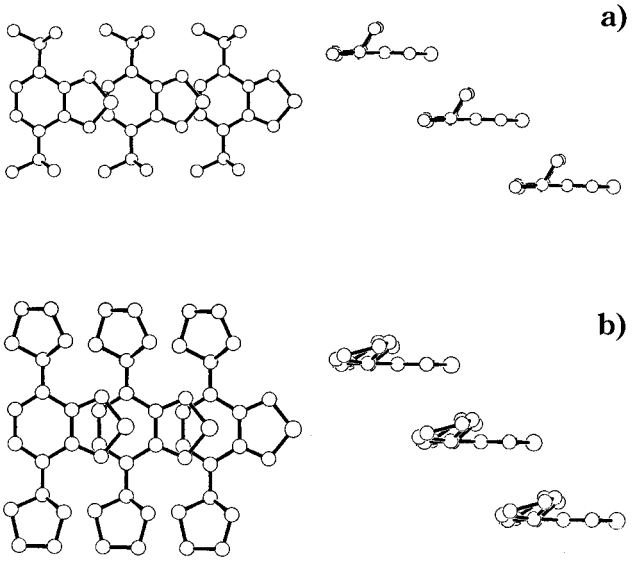

Figure 5. One-dimensional columnar stacking arrangement in **2a** (a) and **2b** (b) crystals. Interplanar distances and dihedral angles between neighbors are 3.34 Å and 0° in the former and 3.29 Å and 0° in the latter, respectively.

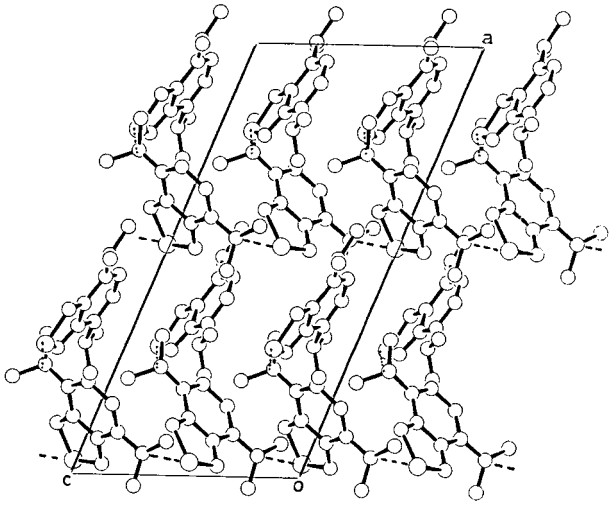

Figure 6. Intermolecular Se···N interaction connecting the molecules of **3a** in crystal. Short contacts of 3.26 and 2.98 Å are indicated by dotted and broken lines, respectively.

of van der Waals radii: 3.55 Å[23]). The former connects two crystallographically independent molecules into a dyad, which is further connected to the neighboring dyads by the latter contacts along the *c* axis to form an infinite array of molecules (Figure 6). These features indicate that the packing arrangement of **3a** is mainly determined by the interheteroatom interaction of Se···N, and changing the chalcogen atom from S to Se causes the drastic difference in crystal structure.[18a]

(19) Saito, G.; Ferraris, J. P. *Bull. Chem. Soc. Jpn.* **1980**, *53*, 2141.
(20) Ueda, N.; Natsume, B.; Yanagiuchi, K.; Sakata, Y.; Enoki, T.; Saito, G.; Inokuchi, H.; Misumi, S. *Bull. Chem. Soc. Jpn.* **1983**, *56*, 775.
(21) Hunter, C. A.; Lawson, K. R.; Perkins, J.; Urch, C. J. *J. Chem. Soc., Perkin Trans. 2* **2001**, 651.

(22) X-ray structural analysis was performed at room temperature (296 K). Detailed geometrical features of **3a** are not discussed in the text due to the relatively large errors for bond lengths (0.004−0.01 Å) and bond angles (0.2−1.0°) as well as the presence of two crystallographically independent molecules. To suppress the large thermal motion of methyl groups and increase the accuracy of the geometrical data, X-ray data collection was also carried out at 223 and 123 K. However, due to the gradual phase transition to structures with lower symmetry (from *Cc*, Z = 8 to *Pc*, Z = 8 then *Pc*, Z = 16), low-temperature structural analyses did not give fruitful results.
(23) Pauling, L. *The Nature of the Chemical Bond*, 3rd ed.; Cornell University Press: Ithaca, NY, 1960; p 260.

Finally, three of the four crystals analyzed here show noncentrosymmetric space groups (**2a**, $P2_12_12_1$; **2e**, $Pna2_1$; **3a**, *Cc*). Although the exact reasons for such polar structures are not clear, they might be promising candidates for nonlinear optical dyes.[24] Studies along these lines are now in progress.

Conclusion

This study has revealed that annelation of the chalcogenadiazole ring to the electron-donating *p*-phenylenediamine skeleton induces several interesting features such as electrochemical amphotericity and intramolecular CT. At the same time, such properties can be easily modified by changing the alkyl substituents on the N_{amino} and/or the chalcogen atom in the heterocyclic moiety. These results show that 4,7-bis(dialkylamino)benzochalcogenadiazoles can be considered a novel class of organic dyes with a wide variety of potential applications in materials chemistry.

Experimental Section

Preparation of 4,7-Bis(dimethylamino)benzo[*c*][1,2,5]-oxadiazole (1a). To a mixture of 35% aqueous HCHO (10 mL) and 3 mol dm^{-3} H_2SO_4 (15 mL) was added dropwise a suspension of $NaBH_4$ 5.23 g (135 mmol) and 4,7-diaminobenzo[*c*][1,2,5]oxadiazole (**1c**)[25] (1.35 g, 9.0 mmol) in THF (30 mL). The whole mixture was then made alkaline by adding NaOH(aq) and extracted with CH_2Cl_2. The combined extracts were washed with brine and dried over Na_2SO_4. Solvent was evaporated and the residue was chromatographed on Al_2O_3 (CH_2Cl_2). Recrystallization from *n*-hexane gave **1a** (1.24 g) as reddish rods in 67% yield: mp 24−26 °C; ^{1}H NMR (200 MHz, $CDCl_3$) δ/ppm 6.18 (2H, s), 3.07 (12H, s); IR (KBr) 2945, 2825, 2780, 1525 cm^{-1}; UV−vis (MeCN) λ_{max} 238 (log ϵ 3.53), 476 (3.55) nm; EI-MS *m*/*z* 206 (M^+). Anal. Calcd for $C_{10}H_{14}N_4O$: C, 58.28; H, 6.84; N, 27.17. Found: C, 58.21; H, 6.66; N, 27.05.

Preparation of 4,7-Bis(1-pyrrolidinyl)benzo[*c*][1,2,5]-oxadiazole (1b). A mixture of amide (**1d**; 180 mg, 0.52 mmol), 1,4-dibromobutane (0.2 mL, 1.6 mmol), and crushed KOH (450 mg, 8.0 mmol) in dry *N*,*N*-dimethylimidazolidinone (10 mL) was heated at 80 °C for 1 h. After adding water (10 mL) and heating again for 20 min, the mixture was diluted with water and extracted with CCl_4. The combined extracts were washed with water and dried over Na_2SO_4. Purification by chromatography (Al_2O_3, CH_2Cl_2/*n*-hexane, 3:1) gave **1b** (35 mg) as red needles in 26% yield: mp 120−122 °C; ^{1}H NMR (90 MHz, $CDCl_3$) δ/ppm 6.00 (2H, broad s), 3.57 (8H, broad); 2.03 (8H, m); IR (KBr) 2950, 2860, 1520 cm^{-1}; UV−vis (MeCN) λ_{max} 242 (log ϵ 4.10), 258 (4.09), 522 (3.47) nm; EI-MS *m*/*z* 259 (M^+ + 1). Anal. Calcd for $C_{14}H_{18}N_4O\cdot(1/4)H_2O$: C, 63.98; H, 7.10; N, 21.32. Found: C, 63.81; H, 6.98; N, 21.16.

Preparation of 4,7-Bis(trifluoroacetylamino)benzo[*c*]-[1,2,5]oxadiazole (1d). A mixture of diamine **1c** (500 mg, 3.0 mmol) and trifluoroacetic anhydride (3.0 mL, 21 mmol) in CCl_4 (15 mL) was heated under reflux for 2 h. After cooling, pale yellow precipitates were filtered and recrystallized from $CHCl_3$ to give **1d** (2.55 g) as pale yellow needles in 73% yield: mp 187−190 °C; ^{1}H NMR (90 MHz, $CDCl_3$) δ/ppm 8.63 (2H, broad s), 8.33 (2H, s); IR (KBr) 3250, 3100, 1727 cm^{-1}; EI-MS *m*/*z* 343 (M^+). Anal. Calcd for $C_{10}H_4N_4O_3F_6$: C, 35.10; H, 1.18; N, 16.37. Found: C, 34.77; H, 1.06; N, 16.64.

Preparation of 4,7-Bis(dimethylamino)benzo[*c*][1,2,5]-thiadiazole (2a). This compound was prepared from diamine **2c** in 63% yield by a procedure similar to that for **1a**: red plates (recrystallization from MeOH), mp 67−68 °C; ^{1}H NMR (200 MHz, $CDCl_3$) δ/ppm 6.63 (2H, s), 3.00 (12H, s); IR (KBr) 2950, 2850, 2825, 2770, 1492 cm^{-1}; UV−vis (MeCN) λ_{max} 262 (log ϵ 4.42), 304 (3.61), 316 (3.48), 478 (3.46) nm; EI-MS *m*/*z* 222 (M^+). Anal. Calcd for $C_{10}H_{14}N_4S$: C, 54.03; H, 6.35; N, 25.20. Found: C, 54.17; H, 6.29; N, 25.07.

Preparation of 4,7-Bis(1-pyrrolidinyl)benzo[*c*][1,2,5]-thiadiazole (2b). A mixture of amide (**2d**; 320 mg, 0.89 mmol), 1,4-dibromobutane (0.23 mL, 2.0 mmol), and crushed KOH (500 mg, 8.9 mmol) in dry acetone (10 mL) was heated at reflux for 2 h. After adding water (10 mL) and heating again for 30 min, the mixture was diluted with water and extracted with CH_2Cl_2. The combined extracts were washed with water and dried over Na_2SO_4. Purification by chromatography (Al_2O_3, benzene) gave **2b** (170 mg) as deep violet needles in 70% yield: mp 111−112 °C; ^{1}H NMR (200 MHz, $CDCl_3$) δ/ppm 6.40 (2H, broad s), 3.60 (8H, broad), 2.02 (8H, m); IR (KBr) 2940, 2850, 2810, 1490 cm^{-1}; UV−vis (MeCN) λ_{max} 270 (log ϵ 4.56), 532 (3.54) nm; EI-MS *m*/*z* 274 (M^+). Anal. Calcd for $C_{14}H_{18}N_4S$: C, 61.28; H, 6.61; N, 20.42. Found: C, 61.34; H, 6.47; N, 20.39.

This material was also prepared in 54% yield through the aldehyde/$NaBH_4$ protocol on diamine **2c** by using 2,5-diethoxytetrahydrofuran as a 1,4-butanedial equivalent.

Preparation of 4,7-Diaminobenzo[*c*][1,2,5]thiadiazole (2c). To a solution of 4-aminobenzo[*c*][1,2,5]thiadiazole (**4c**;[26] 10.0 g, 66.2 mmol) in 0.6 mol dm^{-3} HCl (200 mL) was added portionwise at 0 °C *p*-benzenediazonium sulfonate prepared from 15.7 g (90.8 mmol) of sulfanilic acid and 6.6 g (95 mmol) of $NaNO_2$. After stirring for 2.5 h at 0 °C, dark reddish precipitates of the azo dye were filtered and washed with water and acetone. After drying in vacuo, the well-ground powder was suspended in 3 mol dm^{-3} NaOH(aq) (300 mL). To this solution was added portionwise $Na_2S_2O_4$ (25 g, 144 mmol) at 50 °C, and the mixture was heated at 90 °C for 40 min. After cooling, the mixture was extracted with ether. The ethereal layer was washed with saturated aqueous $NaHCO_3$ and brine and then dried over Na_2SO_4. Purification by chromatography (Al_2O_3,$CHCl_3$) gave **2c** (6.98 g) in 65% yield. Recrystallization from EtOH gave reddish needles: mp 103 °C (dec.); ^{1}H NMR (90 MHz, $CDCl_3$) δ/ppm 6.53 (2H, s), 4.15 (4H, broad s); IR (KBr) 3350, 3150, 1611, 1502, 838 cm^{-1}; EI-MS *m*/*z* 166 (M^+). Anal. Calcd for $C_6H_6N_4S$: C, 43.36; H, 3.64; N, 33.70. Found: C, 43.22; H, 3.60; N, 33.49.

Preparation of 4,7-Bis(trifluoroacetylamino)benzo[*c*]-[1,2,5]thiadiazole (2d). This compound was prepared from diamine **2c** in 84% yield by a procedure similar to that for **1d**: pale yellow crystals (recrystallization from $CHCl_3$); mp 220−221 °C; ^{1}H NMR (90 MHz, $CDCl_3$) δ/ppm 8.94 (2H, broad s), 8.53 (2H, s); IR (KBr) 1700, 1548, 1279, 1267 cm^{-1}; EI-MS *m*/*z* (relative intensity) 358 (M^+, 100), 289 (32), 261 (35). Anal. Calcd for $C_{10}H_4N_4SO_2F_6$: C, 33.53; H, 1.13; N, 15.64. Found: C, 33.45; H, 0.76; N, 15.54.

Preparation of 4-Dimethylamino-7-(1-pyrrolidinyl)-benzo[*c*][1,2,5]thiadiazole (2ab). This compound was prepared from diamine **2bc** in 63% yield by a procedure similar to that for **1a**: violet crystals (Al_2O_3 chromatography, CH_2Cl_2); mp 35−36 °C; ^{1}H NMR (90 MHz, $CDCl_3$) δ/ppm 6.72 (1H, d, J = 7.5 Hz), 6.24 (1H, d, J = 7.5 Hz), 3.72 (4H, m), 3.00 (6H, s), 2.03 (4H, m); IR (KBr) 1570, 1495, 1475, 1390, 1340, 1300 cm^{-1}; UV−vis (MeCN) λ_{max} 268 (log ϵ 4.46), 510 (3.47) nm; EI-MS *m*/*z* (relative intensity) 249 (16), 248 (M^+, 100). Anal. Calcd for $C_{12}H_{16}N_4S$: C, 58.04; H, 6.49; N, 22.56. Found: C, 57.73; H, 6.20; N, 22.52.

Preparation of 4-Amino-7-(1-pyrrolidinyl)benzo[*c*]-[1,2,5]thiadiazole (2bc). This compound was prepared from amine **4b** in 8% yield by a procedure similar to that for **2c** via azo dye: violet crystals (Al_2O_3 chromatography, CH_2Cl_2); mp 53−55 °C; ^{1}H NMR (90 MHz, $CDCl_3$) δ/ppm 6.62 (1H, d, J = 7.5 Hz), 6.25 (1H, d, J = 7.5 Hz), 4.65 (2H, broad s), 3.63 (4H, m), 2.00 (4H, m); IR (KBr) 1590, 1496, 1360, 1328 cm^{-1}; UV−vis (MeCN) λ_{max} 226 (log ϵ 4.40), 522 (3.40) nm; EI-MS *m*/*z* (relative intensity) 220 (M^+, 100), 187 (15), 164 (25). Anal.

(24) Marder, S. R.; Kippelen, B.; Jen, A. K.-Y.; Peyghambarian, N. *Nature* **1997**, *388*, 845.

(25) Borshe, W.; Weber, H. *Liebigs Ann. Chem*. **1931**, *489*, 270.

(26) Efros, L. S.; Levit, R. M. *J. Gen. Chem. (U.S.S.R.)* **1955**, *25*, 183 [cf. *Chem. Abstr.* **1956**, *50*, 1783g].

Calcd for $C_{10}H_{12}N_4S\cdot(1/4)H_2O$: C, 53.43; H, 5.61; N, 24.92; S, 14.26. Found: C, 53.30; H, 5.27; N, 24.61; S, 14.26.

Preparation of 4,7-Bis(dimethylamino)benzo[*c*][1,2,5]-selenadiazole (3a) via 1,2-Diamino-3,6-bis(dimethylamino)benzene (5a). To a solution of **2a** (500 mg, 2.25 mmol) in THF (1 mL) was added dropwise a suspension of $LiAlH_4$ (1.3 g, 34 mmol) in dry THF (8 mL) at 0 °C under N_2. After stirring for 1 h at 0 °C, water-saturated ether (150 mL, degassed) and then 60 mL of degassed water were added. The mixture was extracted with ether under N_2. To the combined extracts containing tetramine (**5a**) was added a solution of SeO_2 (440 mg, 3.37 mmol) in degassed water (20 mL), and the mixture was stirred for 20 h at room temperature under N_2. The mixture was poured into water and extracted with ether. The combined extracts were washed with brine and dried over Na_2SO_4. Chromatographic separation on Al_2O_3 (CH_2Cl_2) followed by recrystallization from *n*-hexane gave **3a** (350 mg) as violet rods in 59% yield.

Data for **3a**. Violet cubes (Al_2O_3 chromatography, CH_2Cl_2); mp 94−94.5 °C; ^{1}H NMR (200 MHz, $CDCl_3$) δ/ppm 6.52 (2H, s), 3.03 (12H, s); IR (KBr) 2920, 2810, 2770, 1480 cm^{-1}; UV−vis (MeCN) λ_{max} 258 (log ϵ 4.18), 324 (3.86), 330 (3.86), 512 (3.38) nm; EI-MS *m*/*z* 270 (M^+). Anal. Calcd for $C_{10}H_{14}N_4Se$: C, 44.62; H, 5.24; N, 20.81. Found: C, 44.53; H, 5.12; N, 20.64.

Data for **5a**. Colorless plates (sublimation), mp 77−80 °C; ^{1}H NMR (90 MHz, $CDCl_3$) δ/ppm 6.57 (2H, s), 3.83 (4H, broad s), 2.65 (12H, s); IR (KBr) 3330, 2920, 2800, 2760, 1495 cm^{-1}; EI-MS *m*/*z* (relative intensity) 194 (M^+, 100), 179 (30), 164 (70), 149 (35). Anal. Calcd for $C_{10}H_{18}N_4$: C, 61.82; H, 9.34; N, 28.83. Found: C, 61.47; H, 9.22; N, 28.64.

Preparation of 4,7-Bis(1-pyrrolidinyl)benzo[*c*][1,2,5]-selenadiazole (3b) via 1,2-Diamino-3,6-bis(1-pyrrolidinyl)benzene (5b). This compound was prepared from thiadiazole derivative **2b** in 34% yield by a procedure similar to that for **3a** via tetramine **5b**.

Data for **3b**. Violet plates (Al_2O_3 chromatography, CH_2Cl_2), mp 101−102 °C; ^{1}H NMR (90 MHz, $CDCl_3$) δ/ppm 6.23 (2H, broad s), 3.57 (8H, broad), 2.03 (8H, m); IR (KBr) 2950, 2800, 1580, 1460, 1390, 1300 cm^{-1}; UV−vis (MeCN) λ_{max} 270 (log ϵ 4.30), 322 (3.82), 580 (3.40) nm; EI-MS *m*/*z* (relative intensity) 321 (M^+, 33), 242 (100). Anal. Calcd for $C_{14}H_{18}N_4Se$: C, 52.34; H, 5.65; N, 17.44. Found: C, 52.08; H, 5.55; N, 17.23.

Data for **5b**. Colorless plates (sublimation), mp 92−94 °C; ^{1}H NMR (90 MHz, $CDCl_3$) δ/ppm 6.45 (2H, s), 2.89 (8H, m), 2.82 (4H, broad s), 1.80 (8H, m); IR (KBr) 3400, 2950, 2810 cm^{-1}; EI-MS *m*/*z* 246 (M^+). Anal. Calcd for $C_{14}H_{22}N_4$: C, 68.26; H, 9.00. Found: C, 68.76; H, 9.09 (correct analytical values could not be obtained due to its instability).

Preparation of 4-(1-Pyrrolidinyl)benzo[*c*][1,2,5]thiadiazole (4b). This compound was prepared from trifluoroamide **4d** in 75% yield by a procedure similar to that for **2b**: orange crystals (Al_2O_3 chromatography, CH_2Cl_2); mp 84−84 °C; ^{1}H NMR (200 MHz, $CDCl_3$) δ/ppm 7.41 (1H, dd, J = 7.5, 8.5 Hz), 7.20 (1H, d, J = 8.5 Hz), 6.23 (1H, d, J = 7.5 Hz), 3.03 (4H, m), 2.06 (4H, m); IR (KBr) 2950, 2820, 1520, 732 cm^{-1}; UV−vis (MeCN) λ_{max} 262 (log ϵ 4.42), 302 (3.53), 314 (3.47), 458 (3.63) nm; EI-MS *m*/*z* 205 (M^+). Anal. Calcd for $C_{10}H_{11}N_3S$: C, 58.51; H, 5.40; N, 20.47. Found: C, 58.60; H, 5.49; N, 20.35.

Preparation of 4-Trifluoroacetylaminobenzo[*c*][1,2,5]-thiadiazole (4d). This compound was prepared from amine **4c**[26] in 78% yield by a procedure similar to that for **1d**: faintly orange plates (recrystallization from petroleum ether); mp 85−88 °C; ^{1}H NMR (90 MHz, $CDCl_3$) δ/ppm 9.13 (1H, broad s), 8.47 (1H, d, J = 8 Hz), 7.80 (1H, dd, J = 8, 8 Hz), 7.61 (1H, d, J = 8 Hz); IR (KBr) 3380, 1725, 1619, 1563, 1144 cm^{-1}; EI-MS *m*/*z* 247 (M^+). Anal. Calcd for $C_8H_4N_3SOF_3$: C, 38.87; H, 1.63; N, 17.00. Found: C, 39.12; H, 1.36; N, 16.93.

Preparation of Crystalline CT Complexes. To a solution of **1a** (50 mg, 0.24 mmol) in CH_2Cl_2 (1 mL) was added a filtered solution of MTDA[18a] (50 mg, 0.19 mmol) in CH_2Cl_2 (10 mL), and the mixture was allowed to stand overnight. Dark green fine needles of the **1a**-MTDA (1:2) complex (57 mg, y. 80%) were filtered and dried in vacuo: mp 150−152 °C (dec.). Anal. Calcd for $C_{10}H_{14}N_4O\cdot(C_{12}H_2N_6S)_2\cdot H_2O$: C, 54.54; H, 2.69; N, 29.93. Found: C, 54.62; H, 2.74; N, 29.56.

Other CT complexes were also obtained by a similar direct method in CH_2Cl_2 or MeCN.

Data for **1a**-BTDA (2:3). Dark green powder, mp 170−200 °C (dec.). Anal. Calcd for $(C_{10}H_{14}N_4O)_2\cdot(C_{12}N_8S_2)_3\cdot 0.5H_2O$: C, 48.65; H, 2.11; N, 32.42. Found: C, 48.50; H, 2.07; N, 32.57.

Data for **2a**-MTDA (1:1). Dark violet powder, mp 133−135 °C (dec.). Anal. Calcd for $C_{10}H_{14}N_4S\cdot C_{12}H_2N_6S$: C, 54.53; H, 3.33; N, 28.91; S. 13.23. Found: C, 53.92; H, 3.32; N, 28.59; S, 13.89.

Data for **2a**-BTDA (1:1). Dark green powder, mp 183−186 °C (dec). Anal. Calcd for $C_{10}H_{14}N_4S\cdot C_{12}N_8S_2$: C, 48.70; H, 2.60; N, 30.98; S. 17.73. Found: C, 48.00; H, 2.73; N, 30.56; S, 17.87.

Data for **3a**-BTDA (1:1). Dark gray powder, mp 170−185 °C (dec.). Anal. Calcd. for $C_{10}H_{14}N_4Se\cdot C_{12}N_8S_2\cdot 0.5H_2O$: C, 44.15; H, 2.53; N, 28.08. Found: C, 44.09; H, 2.55; N, 29.56. Some of the analytical values deviate more than 0.4% from the corresponding calculated value, yet they still support the donor-to-acceptor molar ratios indicated above.

Powder conductivities (σ) were measured in compacted samples by a two-probe method at room temperature. Under the present conditions, σ = 2.7 S cm^{-1} for a TTF-TCNQ complex, a representative molecular metal.

Redox Potential Measurements. Redox potentials (E^{ox} and $E^{red.}$) were measured by cyclic voltammetry in dry MeCN containing 0.1 mol dm^{-3} Et_4NClO_4 as a supporting electrolyte. Ferrocene undergoes 1e-oxidation at +0.38 V under the same conditions. All of the values shown in the text are in *E*/V vs SCE. In the case of irreversible waves, half-wave potentials were estimated from the anodic peak potentials (E^{pa}) as $E^{ox} = E^{pa} - 0.03$ V or the cathodic peak potentials (E^{pc}) as $E^{red} = E^{pc} + 0.03$ V. Although E^{red} of **1e**,[27] **2e**,[28] and **3e**[29] have been reported previously,[3] the values shown in Table 1 were measured under the present conditions for direct comparisons with other compounds.

X-ray Analyses. Crystal data for **2a**. $C_{10}H_{14}N_4S$, *M* 222.31, thin red plate, 0.5 × 0.2 × 0.01 mm (EtOH), orthorhombic $P2_12_12_1$, a = 5.5824(3) Å, b = 19.046(1) Å, c = 10.0343(7) Å, V = 1066.9(1) Å^3, ρ (Z = 4) = 1.384 g cm^{-1}. A total of 1382 unique data ($2\theta_{max}$ = 54.2°) were measured at T = 123 K by a Rigaku Mercury CCD apparatus (Mo Kα radiation, λ = 0.710 69 Å). Absorption correction was applied (μ = 2.75 cm^{-1}). The structure was solved by the direct method (SIR92) and refined by the full-matrix least-squares method on F with anisotropic temperature factors for non-hydrogen atoms. Hydrogen atoms were located at the calculated positions. The final R and Rw values are 0.041 and 0.058 for 1185 reflections with $I > 3\sigma I$ and 136 parameters. Estimated standard deviations are 0.003−0.005 Å for bond lengths and 0.1−0.3° for bond angles.

Crystal data for **2b**. $C_{14}H_{18}N_4S$, *M* 274.38, violet plate, 0.4 × 0.15 × 0.05 mm ($CHCl_3$/*n*-hexane), monoclinic $C2/c$, a = 26.69(2) Å, b = 4.841(4) Å, c = 22.35(2) Å, β = 114.15(1)°, V = 2635(3) Å^3, ρ (Z = 8) = 1.383 g cm^{-1}. A total of 2995 unique data ($2\theta_{max}$ = 54.9°) were measured at T = 123 K by a Rigaku Mercury CCD apparatus (Mo Kα radiation, λ = 0.710 69 Å). Absorption correction was applied (μ = 2.38 cm^{-1}). The structure was solved by the direct method (SIR92) and refined by the full-matrix least-squares method on F with anisotropic temperature factors for non-hydrogen atoms. Hydrogen atoms were located at the calculated positions. The final R and Rw values are 0.079 and 0.097 for 1123 reflections with $I > 3\sigma I$ and 173 parameters. Estimated standard deviations are 0.007−0.01 Å for bond lengths and 0.4−0.7° for bond angles.

Crystal data for **2e**. $C_6H_4N_2S$, *M* 136.17, colorless cube, 0.4 × 0.4 × 0.4 mm (sublimation), orthorhombic $Pna2_1$, a = 12.572(8) Å, b = 12.132(8) Å, c = 3.803(2) Å, V = 580.1(6) Å^3, ρ (Z = 4) = 1.559 g cm^{-1}. A total of 743 unique data ($2\theta_{max}$ = 55.0°) were measured at T = 123 K by a Rigaku Mercury CCD

(27) Zincke, T.; Schwarz, P. *Liebigs Ann. Chem.* **1899**, *307*, 28.
(28) Khaletskii, A. M.; Pesin, V. G. *Z. Obs. Khim.* **1950**, *20*, 1914 [cf. *Chem. Abstr.* **1952**, *46*, 106f].
(29) Bird, C. W.; Cheeseman, G. W. H.; Sarsfield, A. A. *J. Chem. Soc.* **1963**, 4767.

apparatus (Mo Kα radiation, $\lambda = 0.710\,69$ Å). Absorption correction was applied ($\mu = 4.43$ cm^{-1}). The structure was solved by the direct method (SIR92) and refined by the full-matrix least-squares method on F with anisotropic temperature factors for non-hydrogen atoms. Hydrogen atoms were picked up from the D-map and fixed at these positions. The final R and Rw values are 0.029 and 0.042 for 712 reflections with $I > 3\sigma I$ and 83 parameters. Estimated standard deviations are 0.002−0.004 Å for bond lengths and 0.1−0.2° for bond angles.

Crystal data for **3a**. $C_{10}H_{14}N_4Se$, M 269.21, violet cube, 0.35 × 0.30 × 0.20 mm (*n*-hexane), monoclinic *Cc*, $a = 19.764(2)$ Å, $b = 13.557(1)$ Å, $c = 9.584(1)$ Å, $\beta = 112.155(8)°$, $V = 2378.2(4)$ Å^3, ρ ($Z = 8$, two crystallographically independent molecules) = 1.504 g cm^{-1}. A total of 2803 unique data ($2\theta_{max} = 55°$) were measured at $T = 295$ K by a Rigaku AFC-7R four-circle diffractometer with $\omega-2\theta$ scan mode (Mo Kα radiation, $\lambda = 0.710\,69$ Å). Absorption correction was applied ($\mu = 31.33$ cm^{-1}). The structure was solved by the Patterson method and refined by the full-matrix least-squares method on F with anisotropic temperature factors for non-hydrogen atoms. Hydrogen atoms were located at the calculated positions. The final R and Rw values are 0.028 and 0.027 for 2422 reflections with $I > 3\sigma I$ and 269 parameters. Estimated standard deviations are 0.004−0.01 Å for bond lengths and 0.2−1.0° for bond angles.

Acknowledgment. This work was supported by the Ministry of Education, Science and Culture, Japan (Grants 10146101 and 13440184). Financial support from the Izumi Science and Technology Foundation and a Research Grant from the Iwatani Naoji Foundation are gratefully acknowledged. We thank Prof. Tamotsu Inabe (Hokkaido University) for use of the X-ray structure analysis system.

Supporting Information Available: ORTEP drawings (Figures S1−S4) and structural data for the X-ray analyses (positional and thermal parameters, bond distances and angles) of **2a**, **2b**, **2e**, and **3a**. This material is available free of charge via the Internet at http://pubs.acs.org.

JO010808H